Neuron, Vol. 39, 409–421, July 31, 2003, Copyright ©2003 by Cell Press

Triple-Transgenic Model of Alzheimer's Disease with Plaques and Tangles: Intracellular Aβ and Synaptic Dysfunction

Salvatore Oddo,[1] Antonella Caccamo,[1,5] Jason D. Shepherd,[1,5] M. Paul Murphy,[3] Todd E. Golde,[3] Rakez Kayed,[2] Raju Metherate,[1] Mark P. Mattson,[4] Yama Akbari,[1] and Frank M. LaFerla[1,*]

[1] Department of Neurobiology and Behavior
[2] Department of Molecular Biology and Biochemistry
University of California, Irvine
Irvine, California 92697
[3] Department of Neuroscience and Pharmacology
Mayo Clinic Jacksonville
Jacksonville, Florida 32224
[4] Laboratory of Neurosciences
Gerontology Research Center
National Institute on Aging
Baltimore, Maryland 21224

Summary

The neuropathological correlates of Alzheimer's disease (AD) include amyloid-β (Aβ) plaques and neurofibrillary tangles. To study the interaction between Aβ and tau and their effect on synaptic function, we derived a triple-transgenic model (3×Tg-AD) harboring $PS1_{M146V}$, APP_{Swe}, and tau_{P301L} transgenes. Rather than crossing independent lines, we microinjected two transgenes into single-cell embryos from homozygous $PS1_{M146V}$ knockin mice, generating mice with the same genetic background. 3×Tg-AD mice progressively develop plaques and tangles. Synaptic dysfunction, including LTP deficits, manifests in an age-related manner, but before plaque and tangle pathology. Deficits in long-term synaptic plasticity correlate with the accumulation of intraneuronal Aβ. These studies suggest a novel pathogenic role for intraneuronal Aβ with regards to synaptic plasticity. The recapitulation of salient features of AD in these mice clarifies the relationships between Aβ, synaptic dysfunction, and tangles and provides a valuable model for evaluating potential AD therapeutics as the impact on both lesions can be assessed.

Introduction

Alzheimer's disease (AD), a progressive neurodegenerative disorder that is the most common cause of dementia in the elderly, is characterized by two hallmark lesions: diffuse and neuritic plaques, which are predominantly composed of the Aβ peptide, and neurofibrillary tangles, composed of filamentous aggregates of hyperphosphorylated tau protein (Selkoe, 2001). Loss of neuronal synaptic density and synapse number represent another invariant feature of the disease that appears to precede overt neuronal degeneration (DeKosky and Scheff, 1990; Scheff et al., 1991). Notably, the memory and cognitive decline observed in AD patients correlates better with the synaptic pathology than either plaques or tangles, and thus, synaptic dysfunction is likely the most significant factor contributing to the initial stages of memory loss (Dickson et al., 1995; Flood and Coleman, 1990; Masliah et al., 2001; Sze et al., 1997; Terry et al., 1991).

Gene-targeted and transgenic mice have proven to be invaluable for modeling various aspects of AD neuropathology, although no mouse model fully recapitulates its entire neuropathological spectrum (Wong et al., 2002). Numerous models have successfully replicated amyloid plaque deposition, generally by deriving mice with relatively high levels of APP overexpression, and inclusion of a mutant PS1 allele can accelerate the deposition rate as well as exacerbate the pathological severity. The discovery of tau gene mutations in frontotemporal dementia with parkinsonism linked to chromosome 17 kindreds facilitated the development of tauopathies in transgenic mice (Gotz et al., 2001a; Higuchi et al., 2002; Lewis et al., 2000). One surprising aspect of the overwhelming majority of extant AD models has been that the successful development of one hallmark pathological lesion has in and of itself been insufficient to trigger the development of the other signature lesion. Consequently, the concomitant manifestation of both plaques and tangles has required the introduction of multiple transgenes into the same mouse, which has generally been achieved by crossing several independent transgenic lines, or alternatively, by microinjecting pathological protein into the brains of single-transgenic mice (Gotz et al., 2001b; Lewis et al., 2001).

Here, we describe the development of a novel triple-transgenic model (3×Tg-AD). Instead of crossing three independent lines, we derived our transgenic model by directly introducing two additional transgenes into the germline of a genetically modified mouse. We report that (to our knowledge) this is the first transgenic model to develop both plaque and tangle pathology in AD-relevant brain regions. The 3×Tg-AD mice develop extracellular Aβ deposits prior to tangle formation, consistent with the amyloid cascade hypothesis. These mice exhibit deficits in synaptic plasticity, including long-term potentiation (LTP) that occurs prior to extracellular Aβ deposition and tangles but is associated with intracellular Aβ immunoreactivity. Double-transgenic mice (2×Tg) lacking the human APP transgene (but containing $PS1_{M146V}$ and tau_{P301L}) do not develop any extracellular plaques nor do they show any significant intraneuronal Aβ immunoreactivity. Notably, the 2×Tg mice do not exhibit any LTP deficits, despite expressing the tau transgene to comparable levels as the 3×Tg-AD mice. Therefore, such findings suggest a novel pathophysiologic role for intraneuronal Aβ and indicate that synaptic dysfunction is a proximal defect in the pathobiology of AD, preceding extracellular plaque formation and tangles. These 3×Tg-AD mice will be useful for studying the impact of Aβ and tau on synaptic plasticity and for evaluating the efficacy of anti-AD therapies in mitigating

* Correspondence: laferla@uci.edu
[5] These authors contributed equally to this work.

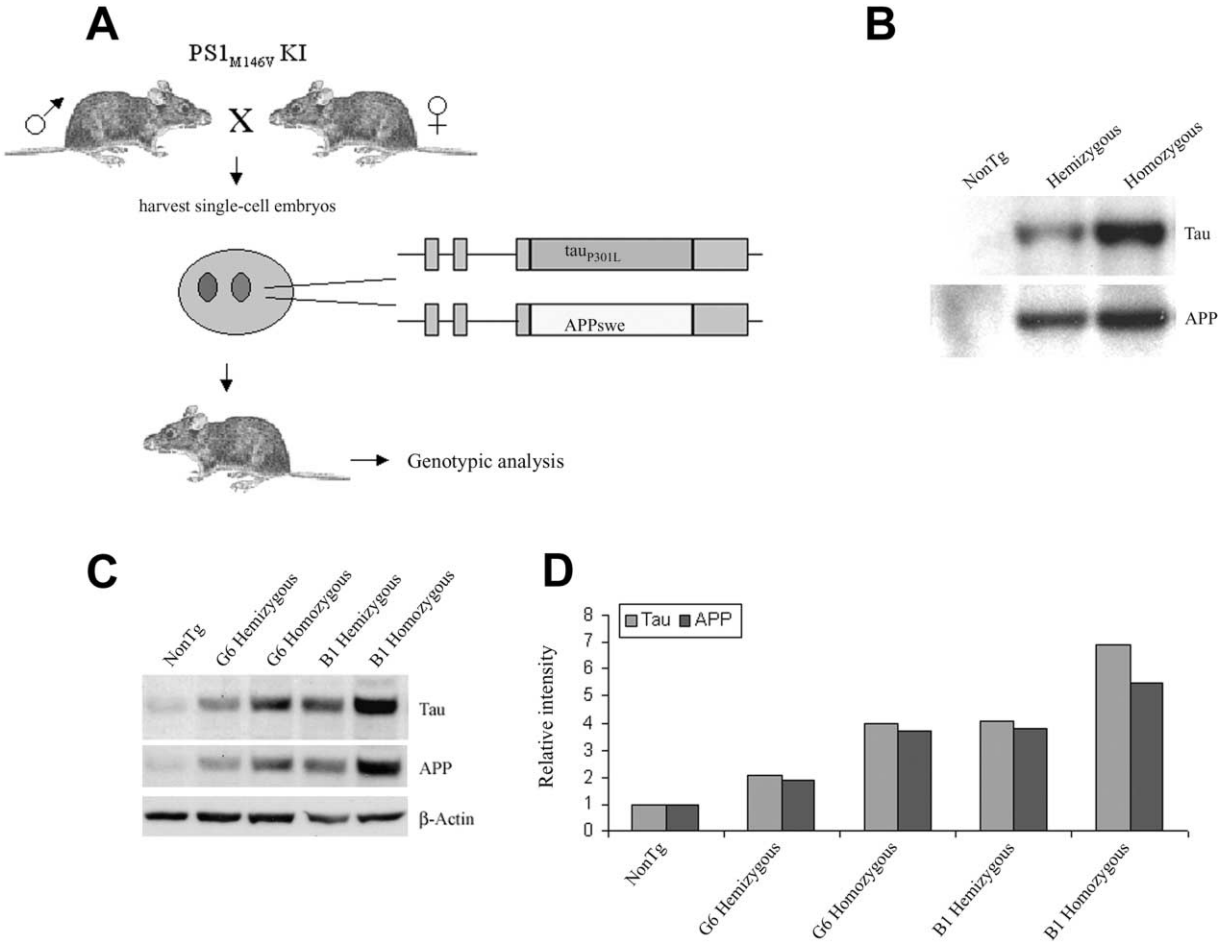

Figure 1. Generation of 3×Tg-AD Mouse Model

(A) Strategy used to develop 3×Tg-AD mice. Using the pronuclear microinjection technique, we coinjected two independent transgene constructs encoding human APP_{Swe} and tau_{P301L} (4R/0N), both under the control of the mouse Thy1.2 regulatory elements, into single-cell embryos harvested from mutant homozygous $PS1_{M146V}$ knockin mice. The entire mouse Thy1.2 genomic sequence is shown with exons depicted as boxes and noncoding sequences as thin lines. The injected embryos were reimplanted into foster mothers and the resulting offspring genotyped to identify 3×Tg-AD mice.

(B) Genotypic analysis for identification of homozygous mice. Representative Southern blot comparing the gene dosage of the human tau and APP transgenes from tail DNA of hemizygous and homozygous mice. Analysis of the transgene transmission frequency confirmed that the mice were homozygous.

(C) Tau and APP expression are doubled in the homozygous mice. Immunoblot comparing steady-state levels of human APP and tau proteins in the brains of 4-month-old hemizygous and homozygous 3×Tg-AD mice from the B1 and G6 lines. For APP (detected with antibody 22C11) and tau (detected with antibody tau5), the levels are doubled in the homozygous mice. Antibodies 22C11 and tau5 recognize both human and mouse APP and tau, respectively.

(D) Steady-state levels of the βAPP and tau protein are approximately 3- to 4-fold and 6- to 8-fold higher than endogenous levels in hemizygous and homozygous mice from the B1 line and 2-fold and 4-fold higher in hemizygous and homozygous mice from the G6 3×Tg-AD line.

the neurodegenerative effects mediated by both signature lesions.

Results

Derivation and Characterization of 3×Tg-AD Mice

Rather than crossing three transgenic lines, we comicroinjected two independent transgenes encoding human APP_{Swe} and human tau_{P301L} (both under control of the mouse Thy1.2 regulatory element) into single-cell embryos harvested from homozygous mutant $PS1_{M146V}$ knockin (PS1-KI) mice (Figure 1A). Because rarely does a single copy of any transgene integrate into a particular locus, we reasoned there was a high probability that the tau and APP transgene cassettes would likely cointegrate into the same site. Six founder lines were identified, five of which were found to harbor all three transgenes. Founder mice were backcrossed to PS1-KI mice. Genotype analysis by Southern blotting indicated that the tau and APP transgenes integrated at the same locus in the majority of the founder lines (data not shown). In at least two lines (B1 and G6), the transgenes appeared to cointegrate at the same locus based on analysis of the transmission frequency, which showed that each transgene did not independently assort in subsequent generations (Table 1). Therefore, comicroinjection of dif-

Table 1. Cotransmission Frequency of the APP and Tau Transgenes in the 3×Tg-AD Lines

Mouse Line	Hemizygous Litters Generated	Number of Offspring (NonTg + Tg)	Number of Transgene Positive Mice	Percent Transgenic	Total Number Coinherited APP and tau	Transgene Cotransmission Frequency
3×Tg-AD B1	30	236	146	61.8%	146	100%
3×Tg-AD G6	8	64	29	45.3%	29	100%
2×Tg A1	13	104	45	43.3%	NA	NA

Analysis of the inheritance pattern of the human tau and APP transgenes in two 3×Tg-AD lines, B1 and G6, revealed that both were inherited with 100% frequency. These data suggest that both transgenes cointegrated at the same locus and, thus, would be transmitted as nonsegregating units. Data from the A1 2×Tg line ($PS1_{M146V}$/Tau_{P301L}) are also shown. All lines were backcrossed to the PS1-KI strain to maintain the M146V mutation.

ferent transgenes appears to be a viable and effective means of generating multitransgenic mice.

Because the APP and tau transgenes cointegrated at the same site and thus are unlikely to independently assort, and because the M146V mutation was "knocked in" to the endogenous mouse PS1 locus (Guo et al., 1999), these 3×Tg-AD mice essentially breed as readily as a "single" transgenic line, even though the mice contain three transgenes. This facilitates the establishment and maintenance of the mouse colony. Moreover, this strategy results in another important pragmatic benefit, as the 3×Tg-AD mice are of the *same* genetic background, thereby reducing a confounding biological variable that is unavoidable when crossing independent transgenic lines.

We next crossed hemizygous F_1 mice to each other to determine if mice homozygous for all three transgenes ($PS1_{M146V}$, tau_{P301L}, APP_{Swe}) could be derived. A doubling of gene dosage is apparent in selected mice by Southern blotting (Figure 1B). These putative homozygous mice were backcrossed to nontransgenic (NonTg) mice and resulted in the expected 100% transmission of the transgenes to the subsequent generation, confirming that the mice were indeed homozygous (data not shown). Homozygous mice were established for both the B1 and G6 lines. Besides further facilitating breeding efforts and the need to genotype the progeny, steady-state levels of human tau and APP transgene products are doubled in the homozygous mice (Figure 1C). Using antibodies that recognize both human and mouse APP or tau, we found that in the B1 line steady-state levels of each transgenic product were ~3- to 4-fold and ~6- to 8-fold higher than endogenous levels in the brains of the hemizygous and homozygous mice, respectively (Figure 1D). Likewise, APP and tau levels were ~2-fold and 4-fold higher in hemizygous and homozygous G6 3×Tg-AD mice (Figure 1D). The maintenance of both hemizygous and homozygous 3×Tg-AD mice renders it possible to study the effect these gene interactions exert as a function of age, in a context in which the expression levels are doubled in mice of the *same* genetic background.

The mouse Thy1.2 expression cassette has been demonstrated to drive transgene expression predominantly to the CNS (Caroni, 1997). Protein extracts from multiple tissues from the B1 3×Tg-AD line (the highest expressing line) were analyzed by Western blot using human-specific antibodies targeted to APP or tau and confirmed that expression was predominantly, if not exclusively, restricted to the CNS (Figure 2A). To determine which regions of the CNS expressed the human APP and tau proteins, we microdissected and prepared protein extracts from multiple brain regions (hippocampus, cortex, cerebellum, etc.) and measured steady-state levels of the transgenic proteins by immunoblotting using human-specific antibodies (Figure 2B). We found that AD-relevant regions, including the hippocampus and cerebral cortex, were among the regions containing the highest steady-state levels of both the transgene-derived human APP and tau proteins. Other regions, such as the cerebellum, did not appear to contain any transgenic proteins, either because they are not expressed there or are rapidly degraded.

To determine whether APP was processed to liberate the Aβ peptide, we analyzed brain homogenates from hemizygous and homozygous mice by immunoprecipitation/Western blotting. Figure 2C shows the presence of a 4 kDa species after probing with an Aβ-derived antibody that is twice as abundant in the homozygous versus hemizygous brains but is undetectable in NonTg brain homogenates. We also compared Aβ40 and Aβ42 levels in the brains of age- and gender-matched NonTg and hemizygous and homozygous 3×Tg-AD mice by sandwich ELISA. There is a progressive increase in Aβ formation as a function of age in the 3×Tg-AD brains and a particularly pronounced effect on Aβ42 levels (Figure 2D). As anticipated, Aβ levels are higher in the homozygous mice relative to the hemizygous mice.

Aβ Precedes Tangle Formation in 3×Tg-AD Mice

Intraneuronal Aβ immunoreactivity is one of the earliest neuropathological manifestations in the both the B1 and G6 3×Tg-AD mice, first detectable in neocortical regions and subsequently in CA1 pyramidal neurons. Intracellular Aβ immunoreactivity is apparent between 3 and 4 months of age in the neocortex of 3×Tg-AD mice (Figure 3A) and by 6 months of age in the CA1 subfield of the hippocampus of hemizygous and homozygous mice (Figure 3D). As with the intraneuronal Aβ immunoreactivity, extracellular Aβ deposits first became apparent in 6-month-old mice in the frontal cortex, predominantly in layers 4 to 5, and were readily evident by 12 months (Figures 3B and 3C). Also by this time point, extracellular Aβ deposits were evident in other cortical regions and in the hippocampus (Figures 3E and 3F), suggesting that there is an age-related, regional dependence to Aβ deposition in the 3×Tg-AD mice. The ELISA data further corroborate the progressive increase in Aβ deposition (Figure 2D).

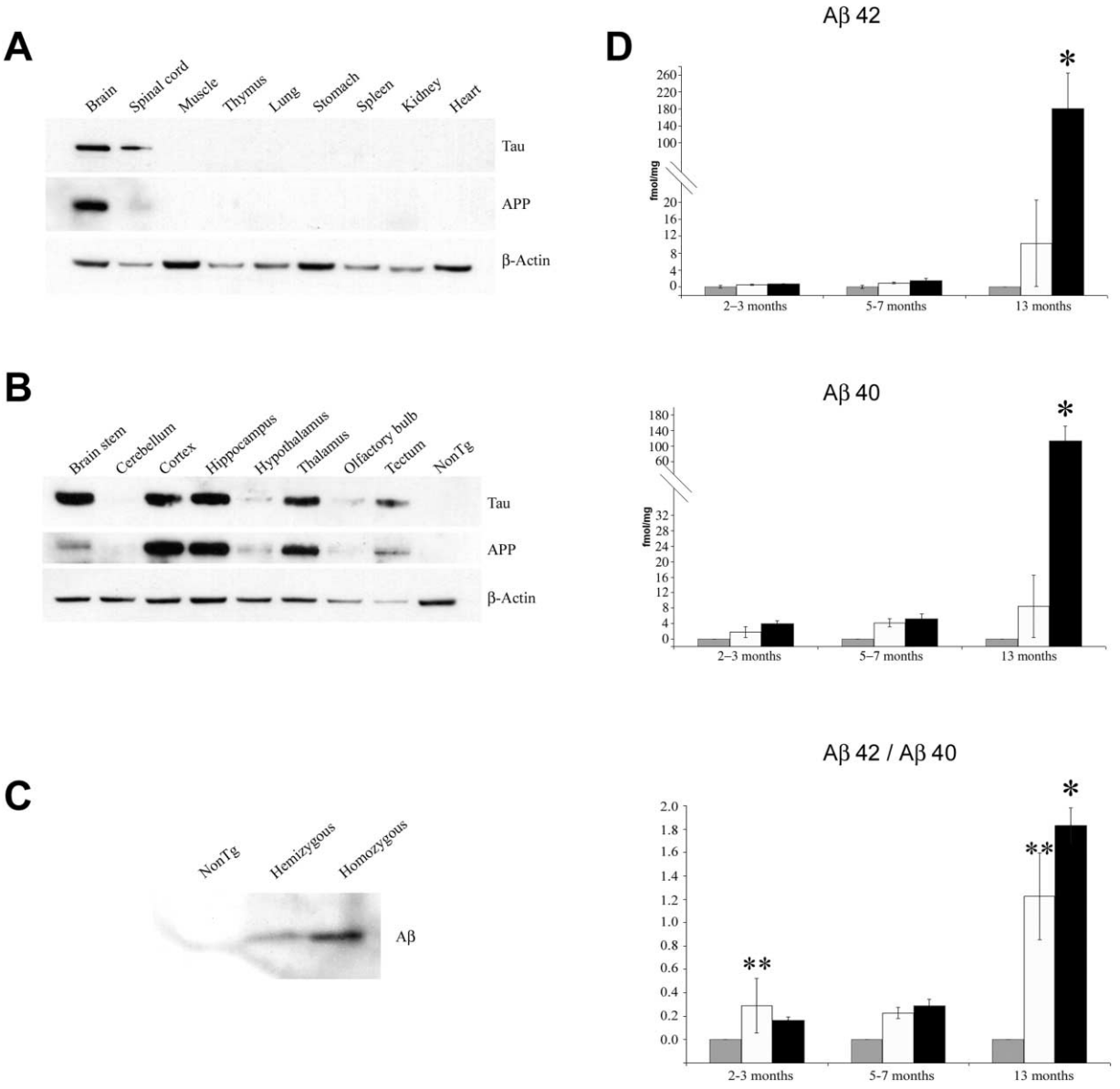

Figure 2. Analysis of Steady-State Levels of the Human Transgene Products in 3×Tg-AD Mice

(A) Multiple peripheral tissues were surveyed by immunoblot analysis to determine the transgene expression profile. Tau and APP appear to be exclusively expressed in the CNS. Antibodies HT7 and 6E10 were used to detect human-specific tau and APP, respectively.

(B) Quantitative comparison of transgene products in various brain subregions by Western blotting with either antibodies HT7 (tau) or 6E10 (Aβ). The hippocampus and cerebral cortex, two prominent AD-afflicted regions, are among the brain regions containing the highest steady-state levels of the human transgene products.

(C) Aβ levels are doubled in the homozygous mice. Immunoprecipitation/Western blotting shows that 4 kDa Aβ is detectable in the brains of both hemizygous and homozygous mice.

(D) Aβ40 and Aβ42 levels were measured by ELISA from different-aged mice (n = 3/group), as described previously (Suzuki et al., 1994). NonTg, hemizygous, and homozygous mice are depicted as gray, white, and black bars, respectively. Statistical difference between hemizygous and NonTg mice is denoted by "**," whereas "*" indicates that homozygous mice are statistically different from hemizygous and NonTg mice.

Although it is difficult to ascertain with complete certainty, based on the use of end-specific Aβ antibodies, some (if not most) of the intracellular immunoreactive material is $A\beta_{42}$ (Figure 4; also see below). The $A\beta_{42}$-specific antibody recognizes many extracellular deposits in the neocortex and hippocampus of mice from the B1 3×Tg-AD line (Figures 4A–4E). This antibody also immunolabels neurons in the hippocampus and cortex of the G6 line as well (Figure 7G). In addition, we show that many of these extracellular Aβ deposits in older mice are also thioflavin S positive (cf. Figures 4E and 4F) and that reactive astrocytes colocalize with some extracellular Aβ deposits (Figure 4G).

Because of the approach used to generate the 3×Tg-AD mice, both the tau and APP transgenes are expressed to comparable levels in the same brain regions.

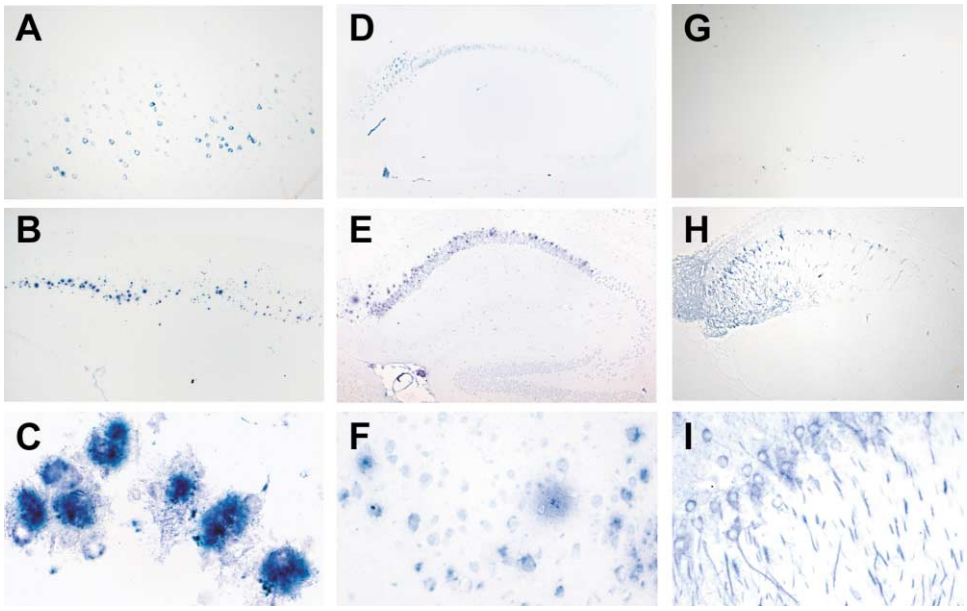

Figure 3. Aβ Deposition Precedes Tau Pathology in 3×Tg-AD Mice

(A) Aβ immunoreactivity is first detected intracellularly in neurons within the neocortex.

(B and C) Low- and high-magnification views, respectively, of the neocortex from a 9-month-old homozygous mouse showing extracellular Aβ deposits in layers 4 to 5 of the neocortex.

(D and E) Hippocampi of homozygous 3×Tg-AD mice (6- and 12-months-old, respectively) showing first intraneuronal Aβ staining in the pyramidal neurons in the CA1 region (D) and then with extracellular Aβ deposits (E).

(F) High-magnification view of section shown in (E).

(G and H) Human tau immunoreactivity, detected with the human-specific anti-tau antibody HT7 is first apparent in the hippocampus and becomes more intense with advancing age (6- to 12-months-old, respectively).

(I) High magnification of section shown in (H). (A)–(F) show Aβ immunoreactivity using monoclonal antibody 1560; (G)–(I) show tau immunostaining with antibody HT7.

Original magnifications: 5× (B, D, E, G, and H), 10× (A), 20× (F and I), and 40× (C).

Consequently, this enabled us to directly test the amyloid cascade hypothesis, which predicts that Aβ is the initiating trigger that underlies all cases of AD (Hardy and Selkoe, 2002). We compared the development of Aβ and tau pathology in 3×Tg-AD mice. Although extracellular Aβ deposits in cortex are apparent by 6 months of age (and even earlier for intracellular Aβ immunoreactivity), no tau alterations are apparent at this age (Figure 3G). It is not until the 3×Tg-AD mice reach about 12 months of age that extensive human tau immunoreactivity is first evident in CA1 neurons, with prominent immunolabeling of the somatodendritic compartments (Figures 3H and 3I). Therefore, despite the comparable overexpression of these two mutant proteins, Aβ pathology develops much earlier than the tau pathology, consistent with the amyloid cascade hypothesis.

Neurofibrillary Alterations

Tau pathology is first apparent in the hippocampus of the 3×Tg-AD, particularly within pyramidal neurons of the CA1 subfield, and then later progresses to involve cortical structures (Figure 5F). This closely mimics the distribution pattern that occurs in human AD brains (Mesulam, 2000). We also confirmed the presence of tau-reactive neurons in the hippocampus and amygdala of 3×Tg-AD mice from the G6 line (Figures 7H and 7I). Conformational- and phospho-specific tau antibodies revealed an age-related progression in alterations of the human tau protein. Conformational-specific antibody MC1 (Figures 5A and 5B) and phospho-tau antibodies AT180, which detects phosphorylated threonine 231 (Figures 5D and 5E); AT8, which detects tau phosphorylated at serine 202 and threonine 205 (Figures 5G and 5H); and PHF1, which detects serine 396 and 404 phosphorylated sites, were used to identify affected neurons (Figures 5K and 5L). Between 12 to 15 months of age, MC1-, AT180-, and AT8-reactive neurons were readily apparent, although staining with PHF1 did not become evident until the mice were about 18 months of age. None of these antibodies bind to normal tau, nor were any of these immunoreactive structures detected in NonTg brains (Figure 5C). Thus, tau is conformationally altered and hyperphosphorylated at multiple residues in the brains of the 3×Tg-AD mice in an age-related and regional-dependent manner. In addition, histological stains, such as Gallayas and thioflavin S, also identify altered tau-reactive neurons, indicating that some of the accumulating tau proteins form aggregates (Figures 5I and 5J).

Tau-reactive dystrophic neurites were also evident surrounding globular structures in older 3×Tg-AD brains (18 months, Figure 5M). These globular structures were thioflavin positive as revealed by analysis of serial sections (cf. Figure 5M with Figure 4F). The 3×Tg-AD mice develop a progressive and age-dependent Aβ and tau pathology, although Aβ deposits manifest prior to tangle

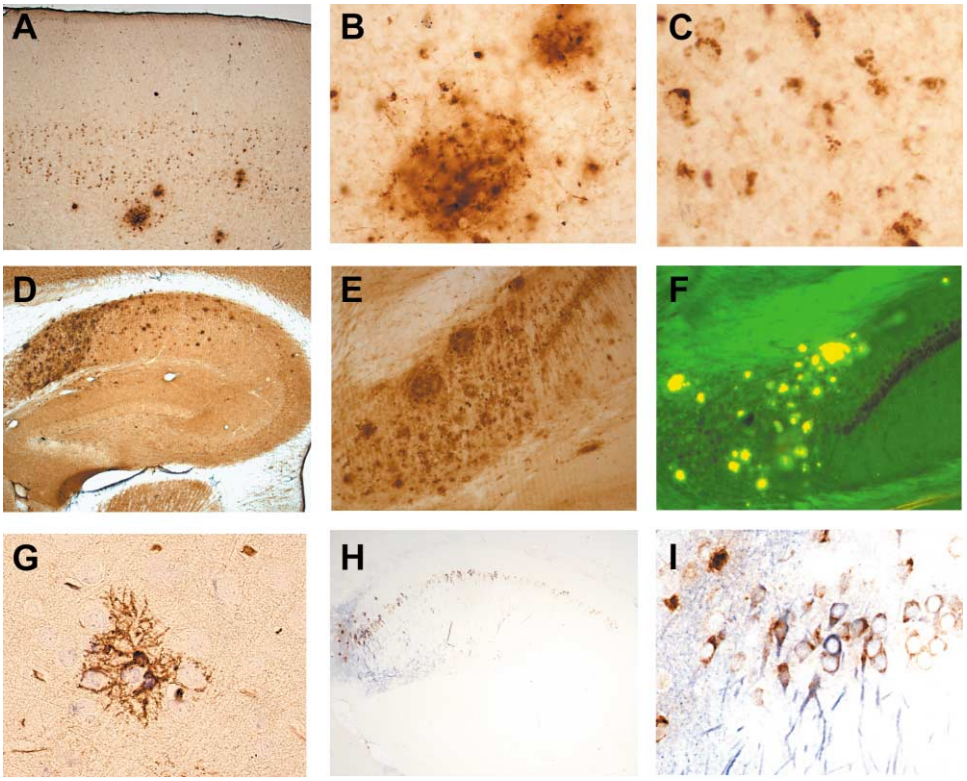

Figure 4. Aβ Deposition Initiates in the Neocortex and Progresses to the Hippocampus

(A) Low-magnification view of neocortex from an aged 3×Tg-AD mouse following staining with Aβ42-specific antibody.

(B and C) Higher-magnification views of section in (A) showing extracellular plaque and intraneuronal Aβ immunoreactivity following staining with Aβ42-specific antibody.

(D) Low-magnification view of hippocampus from 18-month-old 3×Tg-AD mouse with the Aβ42-specific antibody showing the number of Aβ42-reactive plaques.

(E and F) High-magnification view of subicular/CA1 region of panel shown in (D), and (F) a serial section following thioflavin S staining.

(G) Double labeling immunohistochemistry in which astrocytes are reacted with anti-GFAP antibodies and stained brown with DAB, and Aβ is reacted with antibody 6E10 and developed with true blue.

(H and I) Aβ and tau colocalize to many of the same pyramidal neurons. Low- (H) and high- (I) magnification views in which Aβ was immunostained with 6E10 followed by detection with true blue, whereas tau was immunostained with antibody HT7 and detected using DAB (brown staining). Mouse ages are 12 months, (G)—(I), and 18 months, (A)—(F).

Original magnifications: 5× (A and D), 10× (E, F, and H), 20× (B, C, and G), 40× (I).

formation. However, as has been reported, it is likely that Aβ pathology affects the development of tau pathology (Gotz et al., 2001b; Lewis et al., 2001). Although Aβ and tau pathology initiate in different brain regions in the 3×Tg-AD mice (i.e., cortex for Aβ and hippocampus for tau), it is not inconsistent with the notion that Aβ influences tau pathology. The finding that tau and Aβ immunoreactivity colocalize to the same neurons, as revealed by double-labeling immunohistochemistry, further supports the concept that Aβ is poised to influence tau (Figures 4H and 4I). Consequently, it is likely that soluble intracellular Aβ (or an intracellular Aβ-containing APP derivative), which is the first detected pathological manifestation, affects the development of the tau pathology. Aβ42-specific epitopes are also found to be associated with intracellular neurofibrillary tangles in the AD brain (Grundke-Iqbal et al., 1989; Schwab and McGeer, 2000).

Synaptic Dysfunction Is an Early Phenotypic Manifestation

Neuronal and synaptic dysfunction are major phenotypic manifestations of AD neuropathology. Synaptic dysfunction, for example, is among the best correlates for the memory and cognitive changes that characterize AD (DeKosky and Scheff, 1990; Scheff et al., 1991). We compared 1- and 6-month-old homozygous 3×Tg-AD mice to determine if there was an age-related impairment in synaptic function in the CA1 hippocampal region. Age- and gender-matched NonTg and PS1-KI mice were used as controls. PS1-KI mice were evaluated because their electrophysiological properties were unknown and because the 3×Tg-AD mice were directly derived from this line. Thus, it was crucial to determine the effect of the PS1 mutation on synaptic function. In addition, the 6 month time point was selected because extracellular Aβ deposits are evident only in the neocortex and not in the CA1 region of the hippocampus, although intracellular Aβ immunoreactivity is apparent. This allowed us to determine the pathobiological significance of the intracellular Aβ species.

To investigate basal synaptic transmission, we generated input/output (I/O) curves by measuring field-excitatory postsynaptic potentials (fEPSPs) elicited in CA1 by stimulation of the Schaffer collaterals at increasing stimulus intensities. The I/O curves between 1-month-

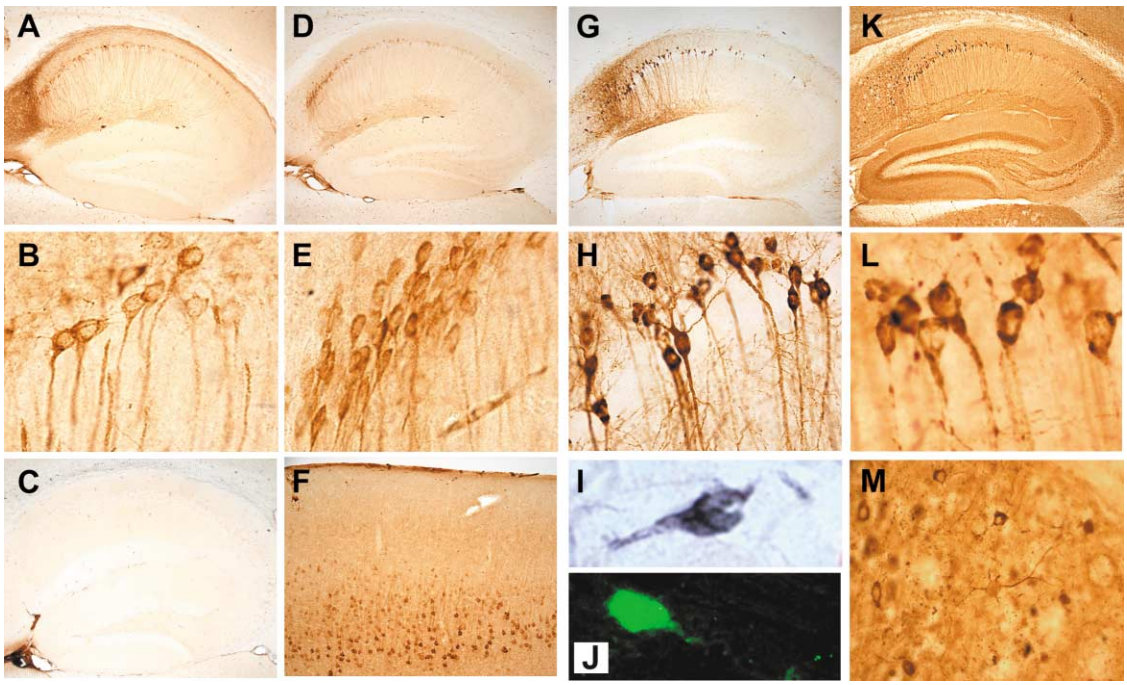

Figure 5. Neurofibrillary Tangles Initiate in the Hippocampus and Progress to the Neocortex

(A and B) Low- and high-magnification views of the hippocampus showing human tau immunopositive pyramidal neurons following staining with the conformational specific antibody MC1.

(C) No altered tau epitopes are present in the hippocampus of NonTg mouse following staining with antibodies HT7, MC1, AT8, AT180, or PHF. Representative section stained with AT8.

(D and E) Low- and high-magnification views of the hippocampus showing tau immunoreactive pyramidal neurons following staining with antibody AT180, which detects phosphorylated tau proteins at threonine 231 residues.

(F) Immunostaining of neocortex with the human-specific tau antibody HT7.

(G and H) Low- and high-magnification view showing immunopositive neurons following staining with antibody AT8, which detects phosphorylated tau proteins at serine 202 and threonine 205 residues.

(I and J) High-magnification view from 12-month-old homozygous mice stained with Gallyas silver stain and thioflavin S, respectively, indicating that the accumulating tau proteins form aggregates.

(K and L) Low- and high-magnification view showing immunopositive neurons following staining with antibody PHF1, which detects serine 396- and 404-phosphorylated residues.

(M) High-magnification view of the subiculum showing tau-reactive dystrophic neurites surrounding globular structures, which are thioflavin-positive Aβ plaques (see Figure 4F).

Original magnifications: 5× (A, C, D, G, and K), 10× (F), 20× (B, E, H, and L), 40× (M), 100× (I and J).

old PS1-KI and 3×Tg-AD mice were not significantly different from NonTg mice (Figure 6A). In contrast, 6-month-old PS1-KI and 3×Tg-AD mice exhibited smaller fEPSP slopes and amplitudes at all stimulus intensities tested and had significantly reduced maximum fEPSPs relative to NonTg mice (Figure 6B). The PS1-KI mice, however, were not significantly different from the 3×Tg-AD mice. These results show that basal synaptic transmission is impaired in both the PS1-KI and 3×Tg-AD mice by 6 months of age.

We investigated paired-pulse facilitation (PPF), a measure of short-term plasticity. No differences in PPF were observed among 1-month-old NonTg, PS1-KI, and 3×Tg-AD mice (Figure 6C). At 6 months of age, there was no difference in the amount of facilitation between NonTg and 3×Tg-AD mice; however, the PS1-KI mice exhibited significantly enhanced PPF compared to NonTg mice (Figure 6D). The mechanisms underlying PPF are thought to be presynaptic (Zucker and Regehr, 2002) and probably involve residual Ca^{2+} in the nerve terminal after the first stimulus, leading to increased neurotransmitter release during the second stimulus (Thomson, 2000). The enhancement of facilitation in the PS1-KI mice may be due to alterations in handling intracellular Ca^{2+} (LaFerla, 2002; Leissring et al., 2000), which can be negated by overexpression of APP in the 3×Tg-AD mice (see below for comment on tau).

Long-term potentiation (LTP), a form of plasticity thought to underlie learning and memory (Bliss and Collingridge, 1993), was investigated in the CA1 hippocampal region. No differences were observed among any of the mouse lines at 1 month of age (Figure 6E). We investigated LTP in 6-month-old 3×Tg-AD mice. Our initial experiments showed that LTP was severely impaired in the 3×Tg-AD mice. However, because the LTP induction protocol used a stimulus intensity that elicited ~30% of the maximum fEPSP slope during baseline, it is plausible that the smaller absolute fEPSP may account for the LTP deficits. To address this possibility, in some experiments, we increased the stimulus intensity of the 3×Tg-AD mice to match baseline fEPSP magnitudes to those of NonTg mice. The stimulus intensity used to elicit LTP in the NonTg sections was approximately 30% of the maximum fEPSP slopes, equating to a value of

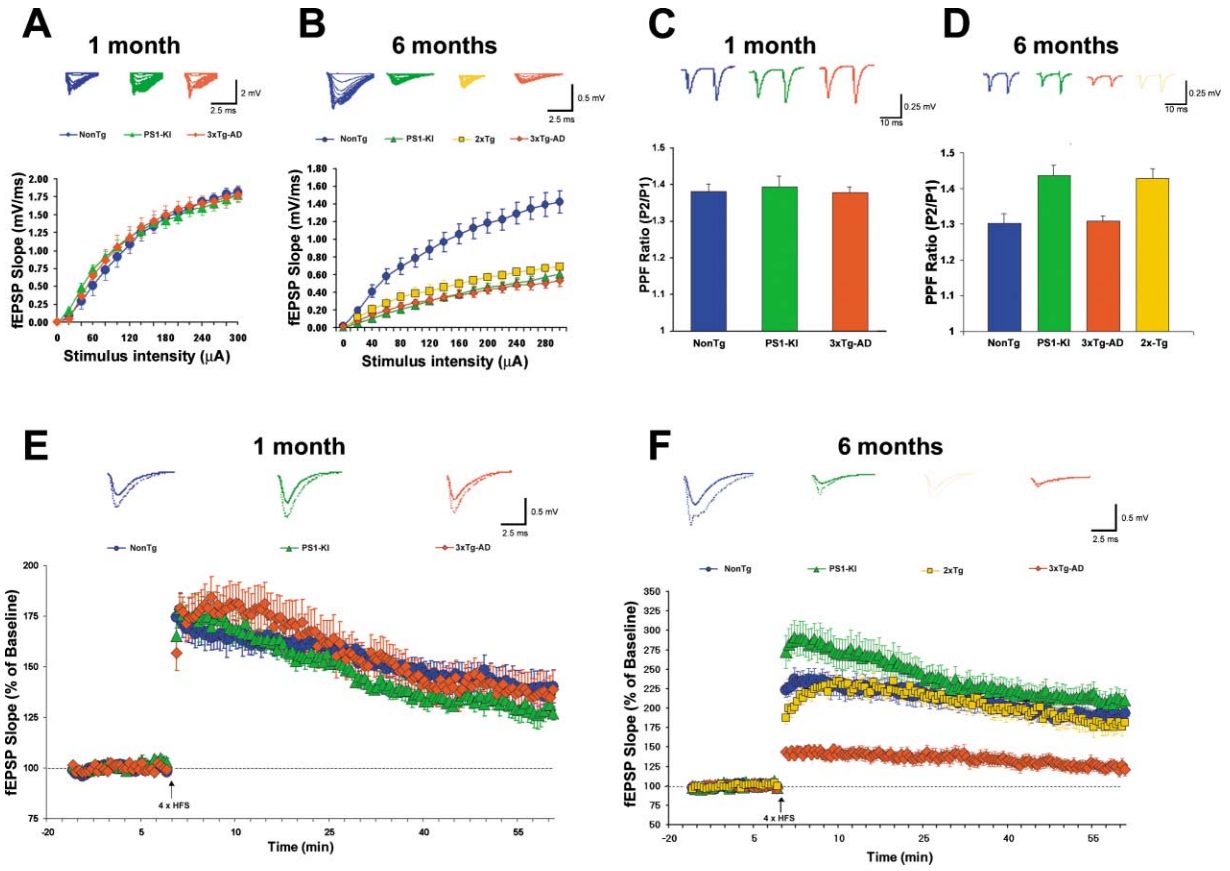

Figure 6. Age-Related Synaptic Dysfunction in 3×Tg-AD Mice

(A) Input/output (I/O) curves and representative fEPSPs at increasing stimulus strengths are shown for NonTg, PS1-KI, and 3×Tg-AD mice, showing no differences at 1 month of age.

(B) Smaller fEPSPs are evoked in six-month-old PS1-KI, tau-PS1 double-transgenic, and 3×Tg-AD mice compared to NonTg mice, indicating impaired synaptic transmission. NonTg, 1.42mV/ms ± 0.17mV/ms, n = 12 slices from six mice; PS1-KI, 0.60mV/ms ± 0.06mV/ms, in n = 14/8, $p < 0.001$; tau-PS1, 0.69 ± 0.05, n = 7/3; 3×Tg-AD, 0.53mV/ms ± 0.06mV/ms, n = 14/6, $p < 0.001$.

(C) Paired-pulse facilitation (PPF) was measured at an interpulse interval of 50 ms and was normal for all groups at 1 month of age.

(D) At 6 months of age, 3×Tg-AD mice exhibited normal PPF compared to NonTg mice (NonTg, 31% ± 1.5%; 3×Tg-AD 30% ± 2.7%, $p < 0.5$), but PS1-KI mice exhibited significantly enhanced PPF (44% ± 2.9%, $p < 0.01$). The double-transgenic mice also showed enhanced PPF (43% ± 2.9%), indicating that mutant tau overexpression did not impact the PS1-mediated effect on PPF.

(E) fEPSP slopes were recorded and were expressed as the percentage of the pretetanus baseline. Representative fEPSPs before (solid line) and 60 min after the induction of LTP (dotted line) are shown. LTP was normal in all groups at 1 month of age.

(F) LTP was markedly impaired in 3×Tg-AD mice. In contrast, short-term LTP was enhanced in PS1-KI mice but was otherwise normal. The amount of potentiation of fEPSPs between 0 and 10 min after HFS was 232% ± 13% in NonTg mice (n = 12/6) and was significantly higher in PS1-KI mice (282% ± 19%, n = 14/8, $p < 0.05$) but was significantly reduced in 3×Tg-AD mice (143% ± 6%, n = 14/6, $p < 0.001$). LTP in the 2×Tg double-transgenic mice was normal and similar to that observed in the NonTg mice, but both groups were significantly lower than PS1-KI mice (219% ± 6%, n = 7/3). The amount of potentiation between 50 to 60 min after HFS was 190% ± 11% in NonTg mice and was not significantly different in PS1-KI mice (212% ± 13%, $p < 0.1$) or 2×Tg mice (182% ± 12%, $p < 0.1$) but was significantly reduced in 3×Tg-AD mice (125% ± 8%, $p < 0.001$).

~0.45mV/ms, which is below the max value of the 3×Tg-AD and PS1-KI mice. LTP magnitudes in these experiments did not significantly differ in the percentage of potentiation when these stronger stimulus intensities were used (nonraised 115% ± 11%, n = 8/4; raised 139% ± 10%, n = 6/2, $p < 0.06$), indicating that reduced basal transmission does not likely account for the deficits in LTP in the 3×Tg-AD mice. In some experiments, we also lowered the baseline fEPSP of the NonTg mice to match 3×Tg-AD mice and found no difference in potentiation as compared with the normal LTP protocol (data not shown). We therefore pooled all the data from the 3×Tg-AD experiments, where baseline fEPSPs were matched to NonTg levels, with the experiments where the normal LTP protocol was used. We also pooled the data from the NonTg experiments, where baseline fEPSPs were lowered to 3×Tg-AD levels, with data from the normal LTP protocol. The pooled data show reduced LTP in the 3×Tg-AD as compared to NonTg mice (Figure 6F). In contrast, in the PS1-KI mice, LTP was essentially normal despite also having weaker fEPSPs relative to NonTg controls (Figure 6B). There was, however, a trend in the PS1-KI mice for significantly higher potentiation during the first 10 min after HFS, as also reported in transgenic mice overexpressing the $PS1_{A246E}$ variant (Parent et al., 1999). As with the 3×Tg-AD mice, raising

baseline fEPSPs to NonTg levels did not result in significantly different LTP, and thus, the data were pooled.

Intracellular Aβ Underlies the Synaptic Dysfunction

One-month-old 3×Tg-AD mice did not exhibit deficits in synaptic plasticity, and likewise, hippocampal brain sections did not show any intracellular Aβ immunoreactivity. At 6 months of age, synaptic dysfunction and LTP deficits were already apparent in the 3×Tg-AD mice. Although no extracellular Aβ deposits are localized to the hippocampal region at this age (Figure 3D), many pyramidal cells in the CA1 subfield were found to be strongly immunoreactive following immunostaining with a variety of antibodies that recognize Aβ epitopes, including antibodies 4G8, 6E10, 1560, and end-specific antibodies that selectively recognize $A\beta_{42}$ (Figure 7B). These data suggest that the intraneuronal accumulation of Aβ underlies the observed synaptic dysfunction. To test this hypothesis, we derived double-transgenic mice (2×Tg) that harbored the human $PS1_{M146V}$ KI mutation and the tau_{P301L} transgene but that lacked the human Swedish APP transgene. As expected, because the 2×Tg mice do not overexpress APP, we could find no evidence of intraneuronal Aβ accumulation (Figure 7C). As with the 3×Tg-AD mice, both hemizygous and homozygous 2×Tg mice were established. We found that the hemizygous 2×Tg mice expressed human tau 6-fold over endogenous mouse tau, comparable to steady-state levels of human tau in the B1 3×Tg-AD homozygous mice (Figure 7D). Therefore, because the expression of PS1 and tau was equivalent between the 2×Tg and 3×Tg-AD mice, we could directly assess the consequences of APP overexpression on synaptic activity between these two transgenic lines.

As shown in Figure 6B, basal synaptic transmission is impaired in the 2×Tg mice to a similar degree as in the PS1-KI and the 3×Tg-AD mice. Notably, PPF in the 2×Tg mice was similar to the PS1-KI mice (Figure 6D), suggesting that expression of mutant tau had no effect on the facilitation mediated by mutant PS1. In contrast, overexpression of APP negates the PS1-mediated effect on PPF (Figure 6D). To determine if LTP was affected in the 2×Tg mice, we directly compared responses in the CA1 hippocampal region to those obtained with the 3×Tg-AD and PS1-KI mice (Figure 6F). We found that the LTP response in the 2×Tg mice was comparable to those observed in NonTg mice, particularly in the maintenance and late phase of LTP. There was, however, a decrease in short-term potentiation as compared to PS1-KI mice, suggesting that overexpression of mutant tau may exert subtle synaptic effects on plasticity. These findings suggest that the pronounced LTP deficits that are apparent in the 3×Tg-AD mice are due to the intracellular accumulation of Aβ. It is evident from these results that the various mutant transgenes all affect synaptic functioning to some degree but that intraneuronal accumulation of Aβ underlies the marked deficit in LTP and also the negative effect on PPF. Acute application of extracellular protofibrillar Aβ has also been shown to modulate LTP in rat brain slices (Walsh et al., 2002). To determine if extracellular protofibrillar Aβ species underlies the synaptic dysfunction in our model, we utilized a novel antibody, A11, that selectively recognizes protofibrillar Aβ species (Kayed et al., 2003). Although we could readily detect protofibrillar Aβ species in the hippocampus of older 3×Tg-AD mice, we failed to detect any extracellular protofibrillar Aβ staining in the 6 month-old mice used for the electrophysiological studies (cf. Figures 7J–7L). Therefore, if there is any extracellular protofibrillar Aβ in the hippocampus at this time point, it occurs below the limit of detection, rendering it unlikely to exert such profound physiological effects, and we conclude that the synaptic dysfunction is likely due to the intraneuronal accumulation of Aβ.

Discussion

We used a novel strategy to develop a triple-transgenic model of AD. Compared to crossbreeding, this approach produces several major advantages. The APP and tau transgenes cointegrated at the *same* genetic locus, rendering it unlikely that either transgene will independently assort in subsequent generations. Consequently, this tight linkage coupled to the knockin of the PS1 mutation indicates that the 3×Tg-AD mice breed as readily as any single-transgenic line, particularly because these mice have also been bred to homozygosity. Thus, deriving a large colony is straightforward, cost effective, and does not require extensive genotyping of the progeny. Moreover, the easy propagation of this transgenic line facilitates their crossing to other transgenic or gene-targeted mice to assess the impact of other genotypes on the neuropathological or physiological phenotype. It is important to note, however, that even the hemizygous mice develop the same neuropathological changes, albeit with a slightly delayed onset. Therefore, crossing these mice to other genetically modified mice does not require returning the original three transgenes to a homozygous state. Finally, another major advantage with this approach is that multiple transgenes are introduced into an animal without altering or mixing the background genetic constitution. Thus, an important confounding variable is avoided, which may be a crucial parameter for behavioral, electrophysiological, and vaccine-based experiments.

The 3×Tg-AD mice that we describe here develop an age-related and progressive neuropathological phenotype that includes both plaque and tangle pathology. Both of these hallmark lesions appear to be mainly restricted to the hippocampus, amygdala, and cerebral cortex—the most pronounced brain structures impacted by AD pathology. In addition, the neuropathology initiates with a regional pattern closely mimicking that observed in AD. Although there is some heterogeneity as to where Aβ first accumulates in the human brain, more often than not, deposition begins in cortical regions and later in the hippocampus. In contrast, tangle formation typically initiates in limbic brain structures and then progresses to cortical regions (Mesulam, 1999). This is precisely the pattern of progression that we observed in the 3×Tg-AD mice. Moreover, the penetrance of the phenotype is 100%, and both male and female mice seem to be equally affected. This latter aspect distinguishes the 3×Tg-AD mice from other models in which one gender seems to be preferentially more vul-

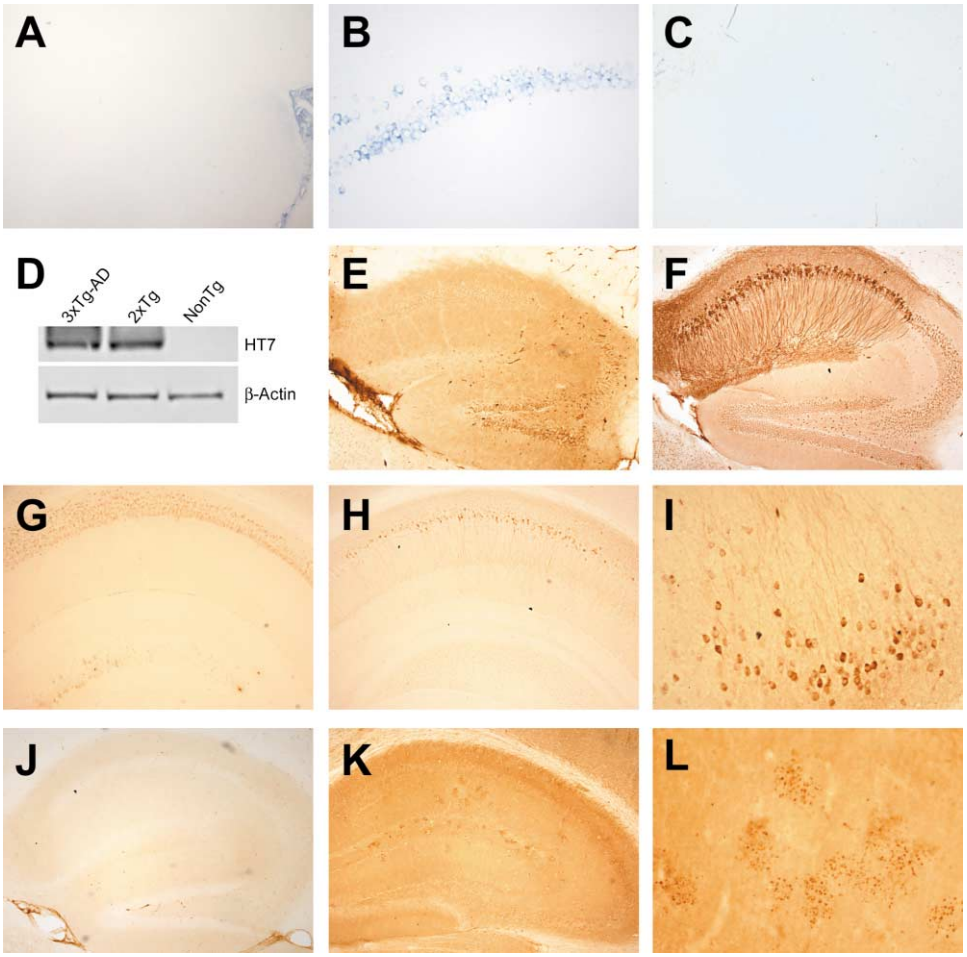

Figure 7. Intraneuronal Aβ Underlies the Synaptic Dysfunction

(A–C) Immunolabeling of hippocampal brain sections with Aβ42-specific antibody in 1- (A) and 6-month- (B) old 3×Tg-AD mice and in 6-month-old 2×Tg mice (C).

(D) Immunoblot showing that steady-state levels of human tau are comparable in the 2×Tg and 3×Tg-AD mice.

(E and F) Despite equivalent expression of human tau protein, the appearance of tau-immunoreactive neurons is delayed in the 2×Tg mice compared to 3×Tg-AD mice. Shown here is an 18-month-old 2×Tg (E) versus a 12-month-old 3×Tg-AD (F) mouse, respectively.

(G–I) Brain sections from 12-month-old G6 3×Tg-AD mouse showing Aβ immunostained neurons in the hippocampus (G) and tau-reactive neurons in the hippocampus (H) and amygdala (I).

(J–L) Protofibrillar Aβ deposits are apparent in older but not younger 3×Tg-AD mice. At 6 months of age, no extracellular protofibrillar Aβ is apparent in the hippocampus, consistent with the synaptic dysfunction being due to intraneuronal Aβ accumulation (J). Low- and high-magnification views of a 12-month-old 3×Tg-AD mouse showing extracellular protofibrillar deposits (K and L).

Original magnifications, 5× (A, G, H, J, and K), 10× (I), 20× (B and M).

nerable (Lewis et al., 2001). The root of this sexual dimorphism between these models is not clear, although differences in the genetic background may be a factor.

Synaptic Plasticity in Alzheimer's Disease

One of the main findings of this study is that synaptic dysfunction is an early change that precedes the accumulation of the hallmark pathological lesions. Another critical finding is that the deficits in synaptic plasticity appear to be triggered by APP overexpression, most likely due to Aβ (see discussion below). Notably, LTP was not significantly impaired in the 2×Tg mice, nor did tau overexpression mitigate the PS1-mediated effects on PPF. Nevertheless, it is probable that altered tau will be found to also affect synaptic plasticity in older transgenic mice.

Mounting evidence points to alterations in synaptic integrity and plasticity as an early phenotypic manifestation in the pathogenesis of AD and specifically to Aβ as the underlying factor that induces changes in synaptic function (see Selkoe [2002] for review). Synapse density is significantly decreased in the AD brain (Terry et al., 1991). Synapse loss, as reflected by changes in the presynaptic marker synaptophysin, correlates better with cognitive deficits than either plaques or tangles (DeKosky and Scheff, 1990; Dickson et al., 1995; Sze et al., 1997; Terry et al., 1991). The 3×Tg-AD mice reported here and other APP models harboring various missense mutations exhibit deficits in basal synaptic transmission, with or without LTP deficits (Chapman et al., 1999; Fitzjohn et al., 2001; Hsia et al., 1999; Moechars et al., 1999). Particular forms of Aβ, which may be differentially

achieved in the various models, may underlie the changes in synaptic efficacy. LTP was inhibited following the intracerebroventricular injection of oligomeric Aβ forms into the rat hippocampus (Walsh et al., 2002), although it is important to consider that the application of exogenously applied Aβ may produce acute effects or involve a different mechanism than that achieved via its gradual buildup with aging. Finally, a recent report finds that neuronal activity can also modulate APP processing; these authors further propose that APP processing and neural activity may be linked through a negative feedback loop (Kamenetz et al., 2003). Therefore, there is increasing appreciation from in vitro and in vivo models for the significant early role that synaptic dysfunction may play in the disease process.

A Pathogenic Role for Intracellular Aβ in Synaptic Plasticity

Intracellular Aβ immunoreactivity is the first clear neuropathological manifestation in the brains of these 3×Tg-AD mice. There is evidence that intracellular Aβ deposition may be important in the pathogenesis of AD (Gouras et al., 2000; LaFerla et al., 1997), Down's syndrome (Gyure et al., 2001), and in the muscle disorder inclusion body myositis (Mendell et al., 1991; Sugarman et al., 2002). Intraneuronal Aβ has also been documented in the brains of other AD-transgenic mouse models (Chui et al., 1999; Kuo et al., 2001; LaFerla et al., 1995; Li et al., 1999; Wirths et al., 2001). Microinjection of nonfibrillar or fibrillar Aβ42 but not Aβ40 in cultured human primary neurons leads to their degeneration, although its extracellular application was without effect (Zhang et al., 2002). The pathophysiological relevance of intraneuronal Aβ in vivo, however, was not clear. Here, we show for the first time (to our knowledge) that the occurrence of intraneuronal Aβ immunoreactivity in CA1 pyramidal neurons correlates with impairments in synaptic plasticity, including deficits in LTP. Immunoelectron microscopic studies show that intraneuronal Aβ42 localizes to multivesicular bodies of neurons within presynaptic and postsynaptic compartments (Takahashi et al., 2002), and it would be interesting to determine if the same occurs in the 3×Tg-AD mice.

The finding that synaptic transmission and LTP deficits precede overt plaque and tangle formation in the 3×Tg-AD mice implies that synaptic dysfunction is an early manifestation of AD and that extracellular Aβ deposition is not the causal factor underlying the synaptic dysfunction. This result agrees with other transgenic studies showing that synaptic transmission can be impacted independent of plaque formation (Hsia et al., 1999). That intracellular Aβ plays a pathogenic role in AD is intriguing. However, it is likely to remain an unsettled topic because of the inherent difficulty in obtaining biochemical confirmation that the putative intracellular species is Aβ and not another Aβ-containing APP derivative or due to contamination. Although it cannot be ruled out that small amounts of extracellular Aβ underlie the synaptic deficits in these mice, this appears to be unlikely because no extracellular Aβ was observed in the hippocampus at the ages used for the physiology experiments, despite using a wide battery of Aβ-specific antibodies (including protofibrillar-specific Aβ antibodies). However, even if some extracellular Aβ is present well below the limit of detection, it is implausible that such miniscule amounts would exert such profound effects on synaptic plasticity. Therefore, based on the preponderance of data, we favor the conclusion that the intraneuronal accumulation of Aβ (or, alternatively, an Aβ-containing APP derivative) contributes to the deficits in synaptic plasticity.

Concluding Remarks

As is the case in human AD, we find that Aβ deposits precede tau alterations in the 3×Tg-AD mice. Because the APP and tau transgenes are expressed to comparable levels, we believe the sequence of neuropathological development in the 3×Tg-AD mice is consistent with the amyloid cascade hypothesis. The fact that these mice overexpress a mutant tau transgene and not the wild-type isoform may complicate the interpretation; however, it is likely that mutant tau will drive the pathology more severely than wild-type tau. Yet, despite this and the equivalent overexpression of the APP and tau transgenes, Aβ pathology still emerges first, where it may be poised to influence the development of the tau neuropathology.

Despite equivalent tau overexpression between the 2×Tg and the 3×Tg-AD mice, the 2×Tg mice do eventually develop tau pathology, although the time frame is significantly delayed with respect to the 3×Tg-AD mice. Likewise, despite the equivalent overexpression of human tau in both models, LTP is not significantly impaired at the age tested, which is not the case for the 3×Tg-AD mice. This finding provides strong evidence that intracellular Aβ accumulation underlies the synaptic dysfunction that occurs in the 3×Tg-AD mice, although subtle synergistic effects with tau cannot be excluded.

The progressive development of both plaques and tangles in an age- and region-dependent manner in the 3×Tg-AD mice has important clinical implications. Besides more closely mimicking the neuropathology of AD, it should help establish if a therapeutic intervention targeted against one of the hallmark lesions is effective at halting or ameliorating the progression of the other. For example, it will be important to determine if clearance of Aβ deposits affect the subsequent development of tangles, as well as its impact on synaptic plasticity.

Experimental Procedures

Generation of 3×Tg-AD Mice

Human APP (695 isoform) cDNA harboring the Swedish double mutation (KM670/671NL) was subcloned into exon 3 of the Thy1.2 expression cassette. Human four-repeat tau without amino terminal inserts (4R0N) harboring the P30IL mutation was also subcloned into Thy1.2 expression cassette. After restriction digestion to liberate the transgene, each fragment was purified by sucrose gradient fractionation, followed by overnight dialysis in injection buffer (10 mM Tris [pH 7.5], 0.25 mM EDTA). Equal molar amounts of each construct were comicroinjected into the pronuclei of single-cell embryos harvested from homozygous $PS1_{M146V}$ knockin mice (Guo et al., 1999). The PS1 knockin mice were originally generated as a hybrid 129/C57BL6 background (Guo et al., 1999). Transgenic mice were identified by Southern blot analysis of tail DNA as described previously (LaFerla et al., 1995; Sugarman et al., 2002). Founder mice were backcrossed to the parental PS1 knockin mice. Both hemizygous and homozygous 3×Tg-AD mice are propagated to study the effects

of increased transgene expression on the neuropathological progression.

ELISAs and Immunoblot

Aβ ELISAs were performed essentially as described previously (Suzuki et al., 1994). For immunoblot, brains from transgenic and control mice were dounce homogenized in a solution of 2% SDS in H_20 containing 0.7 mg/ml Pepstatin A supplemented with complete Mini protease inhibitor tablet (Roche 1836153). The homogenized mixes were briefly sonicated to shear the DNA and centrifuged at 4°C for 1 hr at 100,000 × *g*. The supernatant was used for immunoblot analysis. Proteins were resolved by SDS/PAGE (10% Bis-Tris from Invitrogen) under reducing conditions and transferred to nitrocellulose membrane. The membrane was incubated in a 5% solution of nonfat milk for 1 hr at 20°C. After overnight incubation at 4°C with the primary antibody, the blots were washed in Tween-TBS for 20 min and incubated at 20°C with the secondary antibody. The blots were washed in T-TBS for 20 min and incubated for 5 min with Super Signal (Pierce).

Immunohistochemistry

Formalin-fixed, paraffin-embedded brains were sectioned at 5 μm, mounted onto silane-coated slides and processed as described. The following antibodies were used: anti-Aβ 6E10 and 4G8 (Signet Laboratories, Dedham, MA), anti-Aβ 1560 (Chemicon), A11 (Kayed et al., 2003), anti-APP 22C11 (Chemicon), anti-Tau HT7, AT8, AT180 (Innogenetics), Tau C17 (Santa Cruz), Tau 5 (Calbiochem), anti-GFAP (Dako), and anti-actin (Sigma). Primary antibodies were applied at dilutions of 1:3000 for GFAP; 1:1000 for 6E10; 1:500 for 1560, AT8, AT180, and Tau5; and 1:200 for HT7.

Electrophysiology

Mice were anaesthetized with halothane, decapitated, and the brains were rapidly removed in ice-cold artificial cerebrospinal fluid (aCSF; 125 mM NaCl, 2.5 mM KCl, 1.25 mM KH_2PO_4, 25 mM $NaHCO_3$, 1.2 mM $MgSO_4$, 2 mM $CaCl_2$, and 10 mM dextrose, bubbled with 95% O_2, 5% CO_2 [pH 7.4]). Transverse hippocampal slices (400 μm) were prepared in aCSF using a vibroslice and left to equilibrate for at least 1 hr prior to recording in a holding chamber containing aCSF at room temperature.

Slices were placed in an interface chamber, continuously perfused with aCSF at 34°C, and covered with a continuous flow of warmed humidified gas (95% O_2, 5% CO_2). Field excitatory postsynaptic potentials (fEPSPs) were recorded in the stratum radiatum of the CA1 using glass microelectrodes (1–5Ω, ~ 5 μm diameter) filled with aCSF. Synaptic responses were evoked by stimulation of the Schaffer collateral/commissural pathway with a concentric bipolar stimulating electrode with 0.1 ms pulse width. Input/output curves were generated using stimulus intensities from 0 to 300 μA in increments of 20 μA. PPF was assessed using an interstimulus interval of 50 ms. Baseline fEPSPs were evoked at ~30% of the max fEPSP for 15 min prior to HFS. LTP was induced at baseline intensity using high-frequency stimulation (HFS) consisting of four trains of 100 Hz stimulation at 20 s intervals. Recordings were made every 30 s for 60 min after HFS. The maximum fEPSP slopes were measured offline using Axograph software and were expressed as a percentage of the average slope from the 15 min of baseline recordings. In some experiments, the stimulus intensity was raised so that baseline EPSP slopes matched the average baseline EPSP in the NonTg mice (usually an EPSP ~0.7mV in amplitude). Data were expressed as mean ± SEM and assessed for significance using the Student's t test.

Acknowledgments

We thank P. Caroni for the Thy1.2 expression cassette; M. Hutton for the P301L cDNA; T. Fielder for microinjection of the transgene; C. Glabe for the A11 antibody; and E. Head for advice. J.D.S. was an exchange student from the University of Otago, New Zealand, supported by an Exchange Abroad Scholarship. This work was supported by a grant from the Alzheimer's Association (F.M.L.) and by National Institutes of Health grant AG17968 (F.M.L.).

Received: February 19, 2003
Revised: April 25, 2003
Accepted: May 28, 2003
Published: July 30, 2003

References

Bliss, T.V., and Collingridge, G.L. (1993). A synaptic model of memory: long-term potentiation in the hippocampus. Nature *361*, 31–39.

Caroni, P. (1997). Overexpression of growth-associated proteins in the neurons of adult transgenic mice. J. Neurosci. Methods *71*, 3–9.

Chapman, P.F., White, G.L., Jones, M.W., Cooper-Blacketer, D., Marshall, V.J., Irizarry, M., Younkin, L., Good, M.A., Bliss, T.V., Hyman, B.T., et al. (1999). Impaired synaptic plasticity and learning in aged amyloid precursor protein transgenic mice. Nat. Neurosci. *2*, 271–276.

Chui, D.H., Tanahashi, H., Ozawa, K., Ikeda, S., Checler, F., Ueda, O., Suzuki, H., Araki, W., Inoue, H., Shirotani, K., et al. (1999). Transgenic mice with Alzheimer presenilin 1 mutations show accelerated neurodegeneration without amyloid plaque formation. Nat. Med. *5*, 560–564.

DeKosky, S.T., and Scheff, S.W. (1990). Synapse loss in frontal cortex biopsies in Alzheimer's disease: correlation with cognitive severity. Ann. Neurol. *27*, 457–464.

Dickson, D.W., Crystal, H.A., Bevona, C., Honer, W., Vincent, I., and Davies, P. (1995). Correlations of synaptic and pathological markers with cognition of the elderly. Neurobiol. Aging *16*, 285–304.

Fitzjohn, S.M., Morton, R.A., Kuenzi, F., Rosahl, T.W., Shearman, M., Lewis, H., Smith, D., Reynolds, D.S., Davies, C.H., Collingridge, G.L., et al. (2001). Age-related impairment of synaptic transmission but normal long-term potentiation in transgenic mice that overexpress the human APP695SWE mutant form of amyloid precursor protein. J. Neurosci. *21*, 4691–4698.

Flood, D.G., and Coleman, P.D. (1990). Hippocampal plasticity in normal aging and decreased plasticity in Alzheimer's disease. Prog. Brain Res. *83*, 435–443.

Gotz, J., Chen, F., Barmettler, R., and Nitsch, R.M. (2001a). Tau filament formation in transgenic mice expressing P301L tau. J. Biol. Chem. *276*, 529–534.

Gotz, J., Chen, F., van Dorpe, J., and Nitsch, R.M. (2001b). Formation of neurofibrillary tangles in P301l tau transgenic mice induced by Abeta 42 fibrils. Science *293*, 1491–1495.

Gouras, G.K., Tsai, J., Naslund, J., Vincent, B., Edgar, M., Checler, F., Greenfield, J.P., Haroutunian, V., Buxbaum, J.D., Xu, H., et al. (2000). Intraneuronal Abeta42 accumulation in human brain. Am. J. Pathol. *156*, 15–20.

Grundke-Iqbal, I., Iqbal, K., George, L., Tung, Y.C., Kim, K.S., and Wisniewski, H.M. (1989). Amyloid protein and neurofibrillary tangles coexist in the same neuron in Alzheimer disease. Proc. Natl. Acad. Sci. USA *86*, 2853–2857.

Guo, Q., Fu, W., Sopher, B.L., Miller, M.W., Ware, C.B., Martin, G.M., and Mattson, M.P. (1999). Increased vulnerability of hippocampal neurons to excitotoxic necrosis in presenilin-1 mutant knock-in mice. Nat. Med. *5*, 101–106.

Gyure, K.A., Durham, R., Stewart, W.F., Smialek, J.E., and Troncoso, J.C. (2001). Intraneuronal abeta-amyloid precedes development of amyloid plaques in Down syndrome. Arch. Pathol. Lab. Med. *125*, 489–492.

Hardy, J., and Selkoe, D.J. (2002). The amyloid hypothesis of Alzheimer's disease: progress and problems on the road to therapeutics. Science *297*, 353–356.

Higuchi, M., Ishihara, T., Zhang, B., Hong, M., Andreadis, A., Trojanowski, J., and Lee, V.M. (2002). Transgenic mouse model of tauopathies with glial pathology and nervous system degeneration. Neuron *35*, 433–446.

Hsia, A.Y., Masliah, E., McConlogue, L., Yu, G.Q., Tatsuno, G., Hu, K., Kholodenko, D., Malenka, R.C., Nicoll, R.A., and Mucke, L. (1999). Plaque-independent disruption of neural circuits in Alzheimer's disease mouse models. Proc. Natl. Acad. Sci. USA *96*, 3228–3233.

Kamenetz, F., Tomita, T., Hsieh, H., Seabrook, G., Borchelt, D., Iwatsubo, T., Sisodia, S., and Malinow, R. (2003). APP processing and synaptic function. Neuron *37*, 925–937.

Kayed, R., Head, E., Thompson, J.L., McIntire, T.M., Milton, S.C., Cotman, C.W., and Glabe, C.G. (2003). Common structure of soluble amyloid oligomers implies common mechanism of pathogenesis. Science *300*, 486–489.

Kuo, Y.M., Beach, T.G., Sue, L.I., Scott, S., Layne, K.J., Kokjohn, T.A., Kalback, W.M., Luehrs, D.C., Vishnivetskaya, T.A., Abramowski, D., et al. (2001). The evolution of A beta peptide burden in the APP23 transgenic mice: implications for A beta deposition in Alzheimer disease. Mol. Med. *7*, 609–618.

LaFerla, F.M. (2002). Calcium dyshomeostasis and intracellular signaling in Alzheimer's disease. Nat. Rev. Neurosci. *3*, 862–872.

LaFerla, F.M., Tinkle, B.T., Bieberich, C.J., Haudenschild, C.C., and Jay, G. (1995). The Alzheimer's A beta peptide induces neurodegeneration and apoptotic cell death in transgenic mice. Nat. Genet. *9*, 21–30.

LaFerla, F.M., Troncoso, J.C., Strickland, D.K., Kawas, C.H., and Jay, G. (1997). Neuronal cell death in Alzheimer's disease correlates with apoE uptake and intracellular Abeta stabilization. J. Clin. Invest. *100*, 310–320.

Leissring, M.A., Akbari, Y., Fanger, C.M., Cahalan, M.D., Mattson, M.P., and LaFerla, F.M. (2000). Capacitative calcium entry deficits and elevated luminal calcium content in mutant presenilin-1 knockin mice. J. Cell Biol. *149*, 793–798.

Lewis, J., McGowan, E., Rockwood, J., Melrose, H., Nacharaju, P., Van Slegtenhorst, M., Gwinn-Hardy, K., Paul Murphy, M., Baker, M., Yu, X., et al. (2000). Neurofibrillary tangles, amyotrophy and progressive motor disturbance in mice expressing mutant (P301L) tau protein. Nat. Genet. *25*, 402–405.

Lewis, J., Dickson, D.W., Lin, W.L., Chisholm, L., Corral, A., Jones, G., Yen, S.H., Sahara, N., Skipper, L., Yager, D., et al. (2001). Enhanced neurofibrillary degeneration in transgenic mice expressing mutant tau and APP. Science *293*, 1487–1491.

Li, Q.X., Maynard, C., Cappai, R., McLean, C.A., Cherny, R.A., Lynch, T., Culvenor, J.G., Trevaskis, J., Tanner, J.E., Bailey, K.A., et al. (1999). Intracellular accumulation of detergent-soluble amyloidogenic A beta fragment of Alzheimer's disease precursor protein in the hippocampus of aged transgenic mice. J. Neurochem. *72*, 2479–2487.

Masliah, E., Mallory, M., Alford, M., DeTeresa, R., Hansen, L.A., McKeel, D.W., Jr., and Morris, J.C. (2001). Altered expression of synaptic proteins occurs early during progression of Alzheimer's disease. Neurology *56*, 127–129.

Mendell, J.R., Sahenk, Z., Gales, T., and Paul, L. (1991). Amyloid filaments in inclusion body myositis. Novel findings provide insight into nature of filaments. Arch. Neurol. *48*, 1229–1234.

Mesulam, M.M. (1999). Neuroplasticity failure in Alzheimer's disease: bridging the gap between plaques and tangles. Neuron *24*, 521–529.

Mesulam, M.M. (2000). A plasticity-based theory of the pathogenesis of Alzheimer's disease. Ann. N Y Acad. Sci. *924*, 42–52.

Moechars, D., Dewachter, I., Lorent, K., Reverse, D., Baekelandt, V., Naidu, A., Tesseur, I., Spittaels, K., Haute, C.V., Checler, F., et al. (1999). Early phenotypic changes in transgenic mice that overexpress different mutants of amyloid precursor protein in brain. J. Biol. Chem. *274*, 6483–6492.

Parent, A., Linden, D.J., Sisodia, S.S., and Borchelt, D.R. (1999). Synaptic transmission and hippocampal long-term potentiation in transgenic mice expressing FAD-linked presenilin 1. Neurobiol. Dis. *6*, 56–62.

Scheff, S.W., Scott, S.A., and DeKosky, S.T. (1991). Quantitation of synaptic density in the septal nuclei of young and aged Fischer 344 rats. Neurobiol. Aging *12*, 3–12.

Schwab, C., and McGeer, P.L. (2000). Abeta42-carboxy-terminal-like immunoreactivity is associated with intracellular neurofibrillary tangles and pick bodies. Exp. Neurol. *161*, 527–534.

Selkoe, D.J. (2001). Alzheimer's disease: genes, proteins, and therapy. Physiol. Rev. *81*, 741–766.

Selkoe, D.J. (2002). Alzheimer's disease is a synaptic failure. Science *298*, 789–791.

Sugarman, M.C., Yamasaki, T.R., Oddo, S., Echegoyen, J.C., Murphy, M.P., Golde, T.E., Jannatipour, M., Leissring, M.A., and LaFerla, F.M. (2002). Inclusion body myositis-like phenotype induced by transgenic overexpression of beta APP in skeletal muscle. Proc. Natl. Acad. Sci. USA *99*, 6334–6339.

Suzuki, N., Cheung, T.T., Cai, X.D., Odaka, A., Otvos, L., Jr., Eckman, C., Golde, T.E., and Younkin, S.G. (1994). An increased percentage of long amyloid beta protein secreted by familial amyloid beta protein precursor (beta APP717) mutants. Science *264*, 1336–1340.

Sze, C.I., Troncoso, J.C., Kawas, C., Mouton, P., Price, D.L., and Martin, L.J. (1997). Loss of the presynaptic vesicle protein synaptophysin in hippocampus correlates with cognitive decline in Alzheimer disease. J. Neuropathol. Exp. Neurol. *56*, 933–944.

Takahashi, R.H., Milner, T.A., Li, F., Nam, E.E., Edgar, M.A., Yamaguchi, H., Beal, M.F., Xu, H., Greengard, P., and Gouras, G.K. (2002). Intraneuronal Alzheimer abeta42 accumulates in multivesicular bodies and is associated with synaptic pathology. Am. J. Pathol. *161*, 1869–1879.

Terry, R.D., Masliah, E., Salmon, D.P., Butters, N., DeTeresa, R., Hill, R., Hansen, L.A., and Katzman, R. (1991). Physical basis of cognitive alterations in Alzheimer's disease: synapse loss is the major correlate of cognitive impairment. Ann. Neurol. *30*, 572–580.

Thomson, A.M. (2000). Facilitation, augmentation and potentiation at central synapses. Trends Neurosci. *23*, 305–312.

Walsh, D.M., Klyubin, I., Fadeeva, J.V., Cullen, W.K., Anwyl, R., Wolfe, M.S., Rowan, M.J., and Selkoe, D.J. (2002). Naturally secreted oligomers of amyloid beta protein potently inhibit hippocampal long-term potentiation in vivo. Nature *416*, 535–539.

Wirths, O., Multhaup, G., Czech, C., Blanchard, V., Moussaoui, S., Tremp, G., Pradier, L., Beyreuther, K., and Bayer, T.A. (2001). Intraneuronal Abeta accumulation precedes plaque formation in beta-amyloid precursor protein and presenilin-1 double-transgenic mice. Neurosci. Lett. *306*, 116–120.

Wong, P.C., Cai, H., Borchelt, D.R., and Price, D.L. (2002). Genetically engineered mouse models of neurodegenerative diseases. Nat. Neurosci. *5*, 633–639.

Zhang, Y., McLaughlin, R., Goodyer, C., and LeBlanc, A. (2002). Selective cytotoxicity of intracellular amyloid beta peptide1–42 through p53 and Bax in cultured primary human neurons. J. Cell Biol. *156*, 519–529.

Zucker, R.S., and Regehr, W.G. (2002). Short-term synaptic plasticity. Annu. Rev. Physiol. *64*, 355–405.